

Supporting Information of

Gravity Wave Parameters and Their Seasonal Variations Study near 120°E China Based on Na LIDAR Observations

Xu Zou ^{1,2,3,4}, Guotao Yang ^{2,3,*}, P. P. Batista ⁵, Jihong Wang ², V. F. Andrioli ^{3,5}
Xuewu Cheng ⁶, Jing Jiao ^{2,3}, Lifang Du ², Tiemin Zhang ^{1,4}, Hong Yang ^{1,4},
Zelong Wang ⁷ and Yuan Xia ⁸

¹ College of Physics & Electronics Engineering, Hainan Normal University, Haikou 571158, China

² State Key Laboratory of Space Weather, National Space Science Center, CAS, Beijing 100011, China

³ China-Brazil Joint Laboratory for Space Weather, CAS, Sao Jose dos Campos 12227-010, Brazil

⁴ Key Laboratory of Laser Technology and Optoelectronic Functional Materials of Hainan Province, Haikou 571158, China

⁵ National Institute for Space Research, INPE, São José dos Campos 12227-010, Brazil

⁶ Innovation Academy for Precision Measurement Science and Technology, CAS, Wuhan 430071, China

⁷ School of Science, Jiangsu University of Science and Technology, Zhenjiang 212003, China

⁸ College of Electronic Engineering, Nanjing Xiaozhuang University, Nanjing 211171, China

* Correspondence: gtyang@swl.ac.cn; Tel:0086-010-62586358.

The fitted value of the atmospheric density perturbation seasonal distribution

The fitted value of the atmospheric density perturbation with their annual, semiannual component are calculated by MMSE fit which was shown in Table S1~S3.

Table S1. Fitted Components of GW Parameters ^a at Beijing at Annual and Semiannual

GW parameter are $y = A_0 + A_1 \cos[2\pi/365(d-d_1)] + A_2 \cos[4\pi/365(d-d_2)]$.

	A ₀	A ₁	A ₂	d ₁	d ₂	A ₁ / A ₀	A ₂ / A ₀	d ₁ -d ₂
$\langle r_a^2 \rangle^{1/2}(\%)$	5.84	0.98	0.72	181	188	0.16	0.12	-7
Fa(m ₈), m/cycles	4.47	1.69	1.21	193	187	0.39	0.27	6
Fa(m ₄), m/cycles	1.20	0.58	0.34	197	187	0.48	0.28	10
Fa(m ₁₅), m/cycles	0.61	0.376	0.207	193	188	0.61	0.34	5
Fa(m ₁), m/cycles	0.013	0.008	0.0045	190	194	0.60	0.33	-4
Fa(ω ₆₀), s/cycles	1.34,	0.786	0.67	174,	193	0.59	0.50,	-19
Fa(ω ₄₅), s/cycles	0.761,	0.51,	0.37,	180	188	0.67	0.49	-8
Fa(ω ₁₅), s/cycles	0.124	0.093	0.052	179	186	0.75	0.41	-7

^a A₀ denotes Mean value of parameters; d is short for “day”

A₁: Annual Amplitude; A₂: Semiannual Amplitude; d₁: Annual Phase; d₂: Semiannual Phase

Table S2. Annual and Semiannual Components of Gravity Wave Parameters at Hefei

	A ₀	A ₁	A ₂	d ₁	d ₂	A ₁ / A ₀	A ₂ / A ₀	d ₁ -d ₂
$\langle \Gamma_a^2 \rangle^{1/2}(\%)$	7.84	1.02	1.3	-32	-5	0.13	0.17	-27
Fa(m ₈), m/cycles	10.29	4.03	5.34	-19	-3	0.39	0.52	-16
Fa(m ₄), m/cycles	3.05	1.39	1.46	-19	-8	0.46	0.48	-11
Fa(m ₂), m/cycles	1.05	0.54	0.54	-10	-4	0.51	0.51	-6
Fa(m ₁), m/cycles	0.616	0.32	0.35	-18	-6.5	0.52	0.57	-11.5
Fa(ω_{60}), s/cycles	2.82	1	0.83	13	-13	0.35	0.29	26
Fa(ω_{45}), s/cycles	1.55	0.41	0.47	4	1	0.26	0.30	3
Fa(ω_{15}), s/cycles	0.3	0.2	0.21	-18	-6	0.67	0.70	-12

Table S3. Annual and Semiannual Components of Gravity Wave Parameters at Hainan

	A ₀	A ₁	A ₂	d ₁	d ₂	A ₁ / A ₀	A ₂ / A ₀	d ₁ -d ₂
$\langle \Gamma_a^2 \rangle^{1/2}(\%)$	5.86	0.48	0.57	-72	-9	0.085	0.10	-63
Fa(m ₈), m/cycles	1.69	0.49	0.53	-40	-14	0.29	0.31	-26
Fa(m ₄), m/cycles	0.22	0.10	0.10	-34	-18	0.45	0.45	-16
Fa(m ₂), m/cycles	0.087	0.039	0.039	-26	-15	0.45	0.45	-11
Fa(m ₁), m/cycles	0.02	0.009	0.01	-31	-15	0.45	0.5	-16
Fa(ω_{60}), s/cycles	0.97	-0.23	0.33	-11	-24	-0.24	0.34	13
Fa(ω_{45}), s/cycles	0.70	-0.23,	0.05	18	-17	-0.33	0.07	35
Fa(ω_{25}), s/cycles	0.12	-0.03	-0.05	-30	50	-0.25	-0.42	-80

The Spectra of Vertical Wave Number “Fa(m)” Study

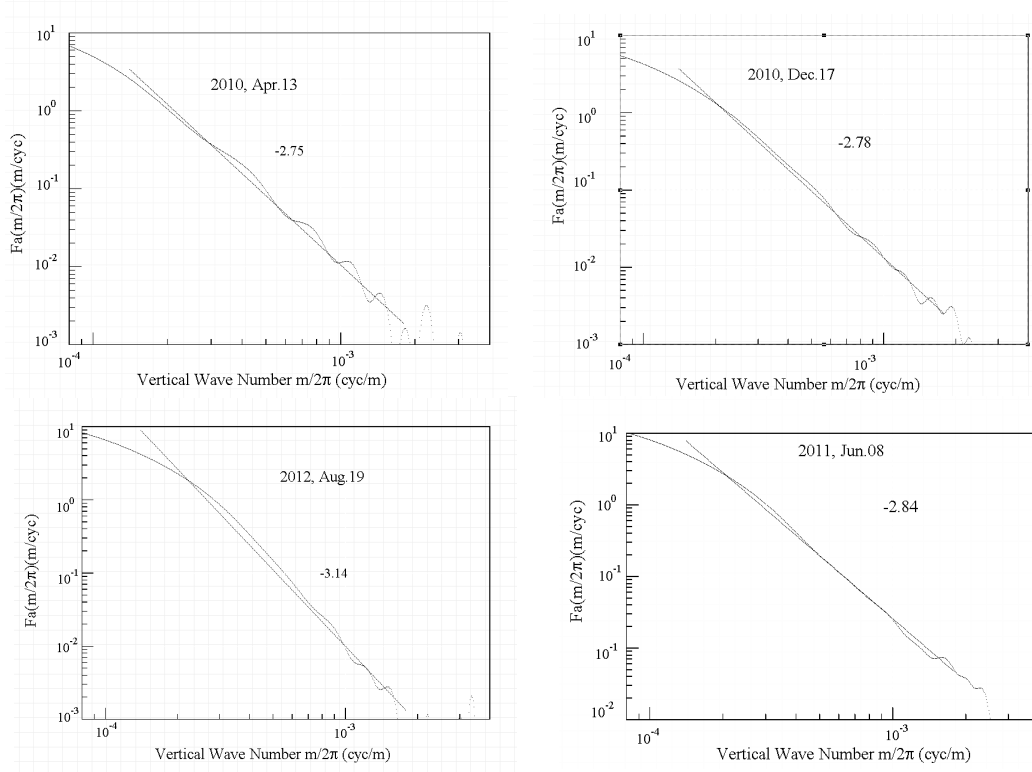


Figure S1. Selected $F_a(m)$ and their fitting slope to the nightly spectra of GW atmospheric density perturbations nightly at **Beijing**.

In order to investigate the GW field energies, vertical wave number spectrum $F_a(m)$ which is also called vertical power spectrum is considered to be the effective method based on analysis of density of atmosphere perturbation. And according to Gardner’s theory, $F_a(m)$ is defined as the spatial Fourier transform of atmospheric density perturbations [Senft and Gardner, 1991; Yang et al., 2006].

$$F_a(m) = \int_{-\infty}^{\infty} B_a(s, 0) e^{ims} ds = \int_{-\infty}^{\infty} \langle r_a(z, t) r_a(z-s, t) \rangle e^{ims} ds$$

For obtaining the better result, the $r_a(z, t)$ should be pre-whitened by function: $y(z, t) = r_a(z, t) - 0.95r_a(z - \Delta z, t)$ firstly, and dealt with a *Hamming window* to modify the result successively as the similar work that was given by Tsuda et al. [1989]. Notably

the photon noise for all the spectra has been subtracted which will make the data more accurate and reliable.

The selected examples of the atmospheric density perturbations $F_a(m)$ and their fitted slope at Beijing were shown in Figure S1. As for the relation of vertical wave number and $F_a(m)$, the units of which were marked as “cyc/m” and “m/cycles” respectively. And it is indicated, obviously, that the $F_a(m)$ are in linear regression relationship with m for the examples. And by statistical of spectral slope, our result is a little higher than the report of Senft and Gardner [1991]. Besides, we also calculated the curve at middle and low-middle latitude (Hefei and Hainan, respectively), which are shown in the given below.

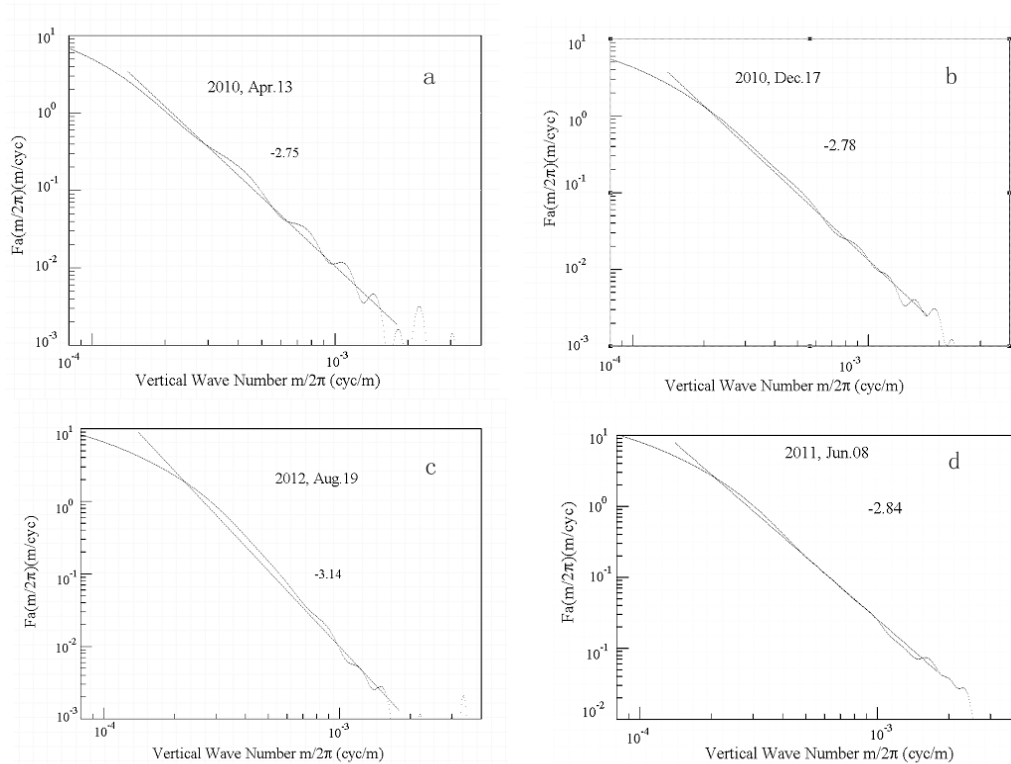


Figure S2. Vertical wave number power spectra of atmospheric density perturbations associated with gravity waves in the menopause region at **Hefei**. The straight dotted lines are the regression fits to the spectra.

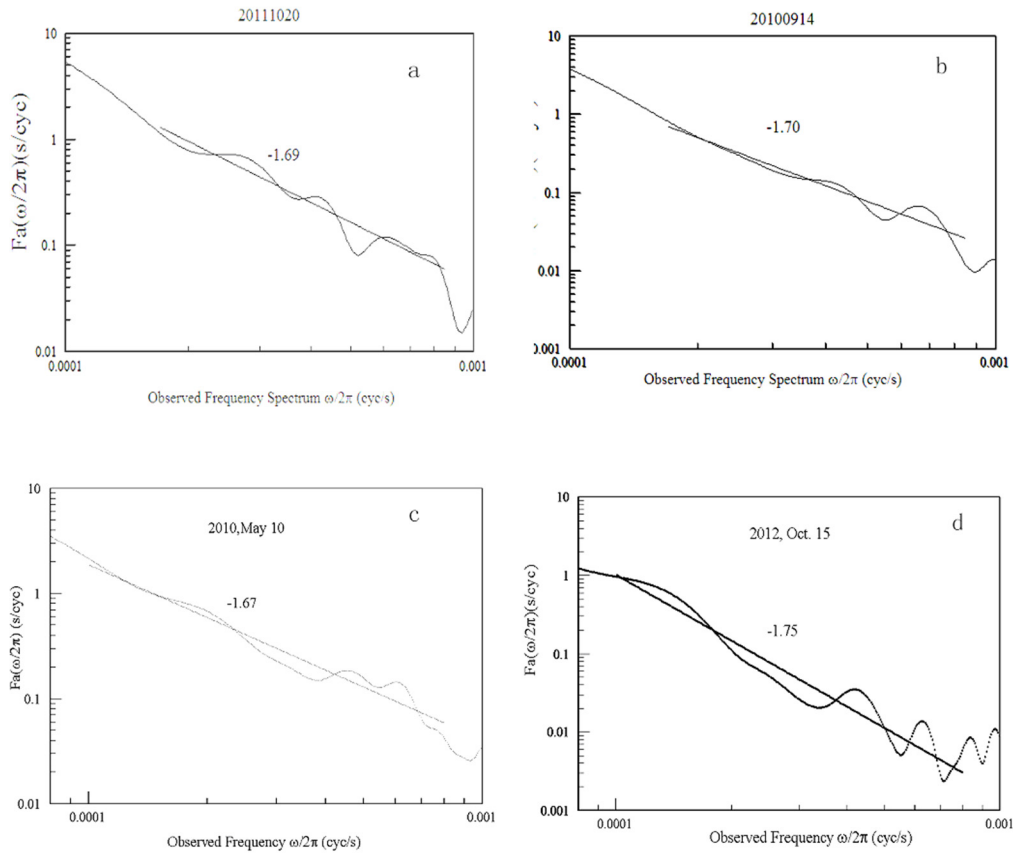


Figure S3. Frequency spectra of atmospheric density perturbations associated with gravity waves in the menopause region at **Hainan**.

The annually averaged $F_a(m)$ at three sites were indicated in **Figure S4**. The fitted linear spectra slope at Beijing is -2.98 , and meanwhile the averaged $F_a(m)$ linear slope value at Hefei and Hainan are -3.02 and -2.93 , respectively. These results are much closed to the Doppler-spreading theory and linear instability theory at a value of -3 as the predictions by Hines [1991] and Dewan and Good, [1986].

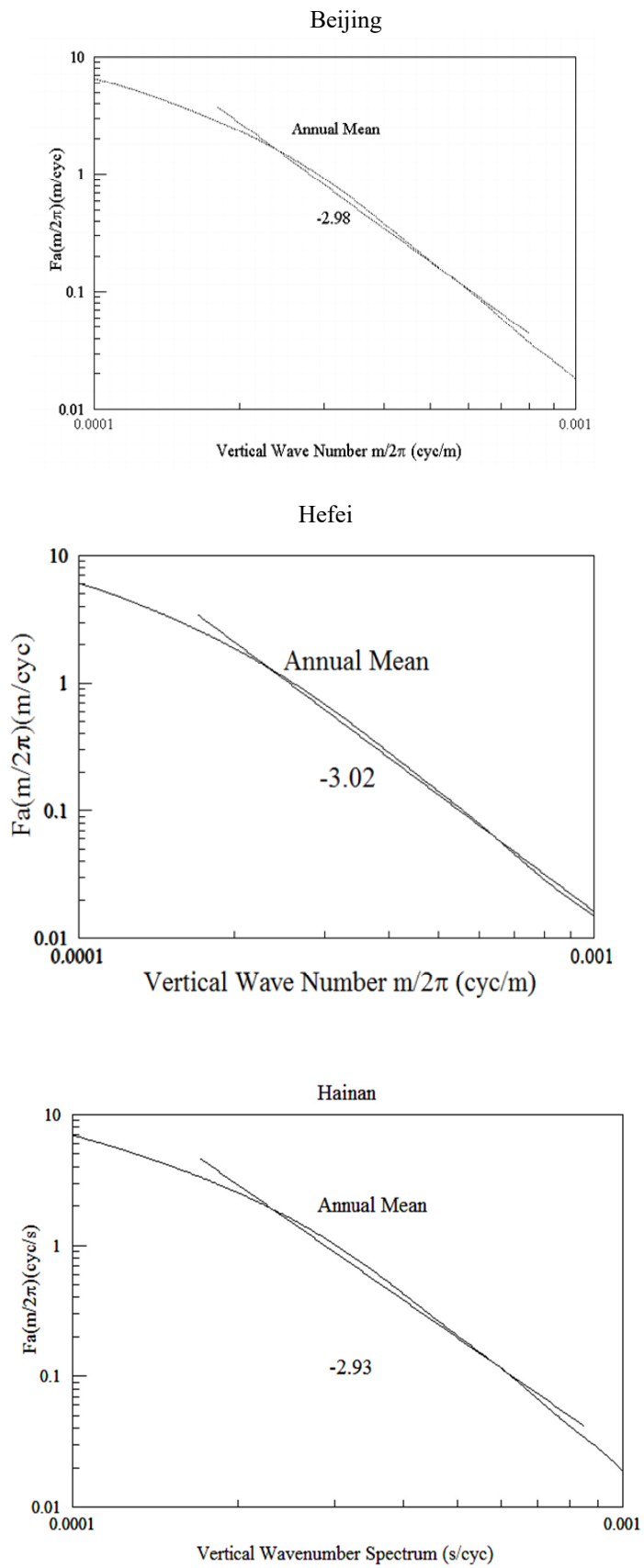


Figure S4. Annual averaged $F_a(m)$ at Beijing (top), Hefei (middle) and Hainan (bottom) .

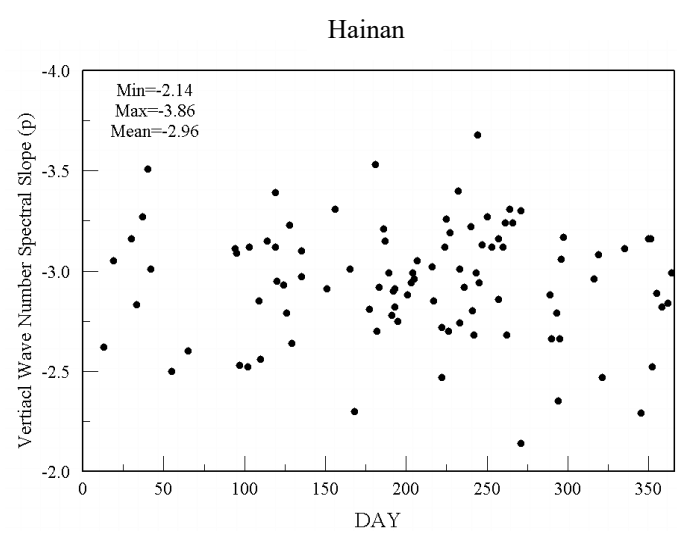
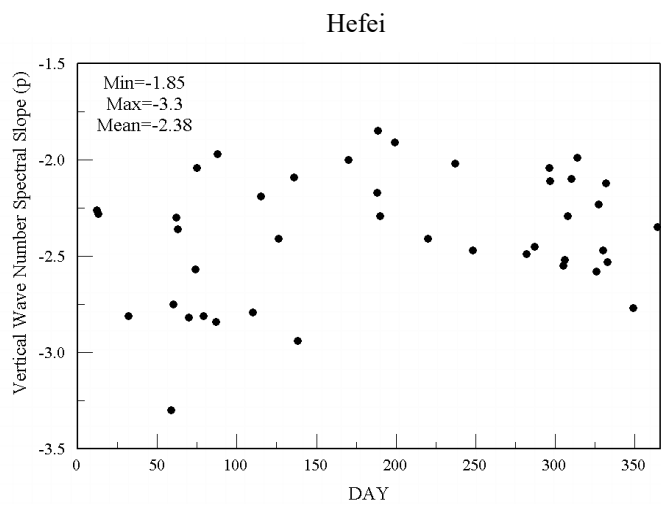
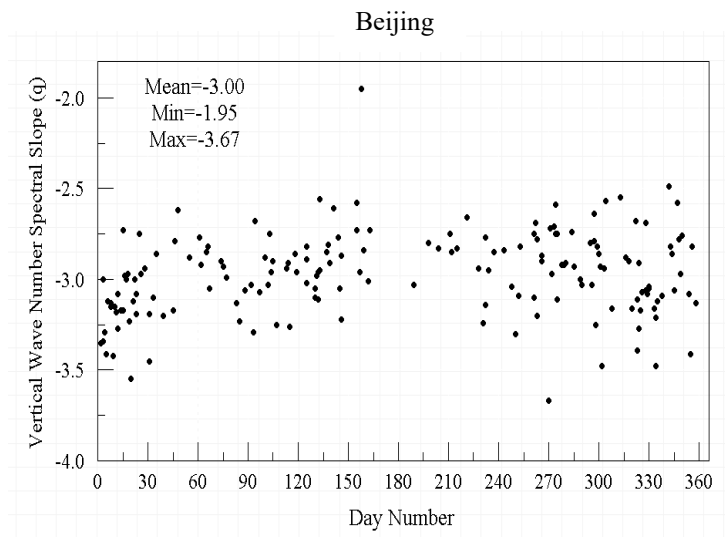


Figure S5. Distribution of the fitted regression spectra slopes $F_a(m)$ at Beijing (top), Hefei (middle) and Hainan (bottom).

And Figure S5 indicated the seasonal distribution of $F_a(m)$ spectral slopes (p) at three sites. At Beijing, the slope values distribute between -1.95 to -3.67 which is consistent with Senft and Gardner [1991]'s report from -2.14 to -3.86 , Senft et al. [1993] has given a slope value range based on only one month of data between -2.1 to -3.5 , not only at mid latitude area, while at the South Pole, Collins et al [1994] reported the shallowest and steepest slope value of -2.0 and -3.5 respectively. While Hainan and Hefei's slopes are also indicated as -1.95 to -3.67 and -1.85 to -3.3 that are similar as the previous reports Senft and Gardner [1991].

The averaged $F_a(m)$ mean slope at three sites are -3.00 (Beijing), -2.38 (Hefei) and -2.93 (Hainan) respectively, which is quite consistent with the aforementioned theory value of -3 , and different with the extreme data -2.4 which was observed at the South Pole by Collins et al. [1994]. That is because the three observatories have a lower inertial frequency so that the obtained slope is larger than the Antarctica observation. While those data as -2.90 and -2.98 that are given by Senft and Gardner [1991] and Beatty et al. [1992] respectively are also both close to our value.

The spectra of observed frequency $F_a(\omega)$ Study

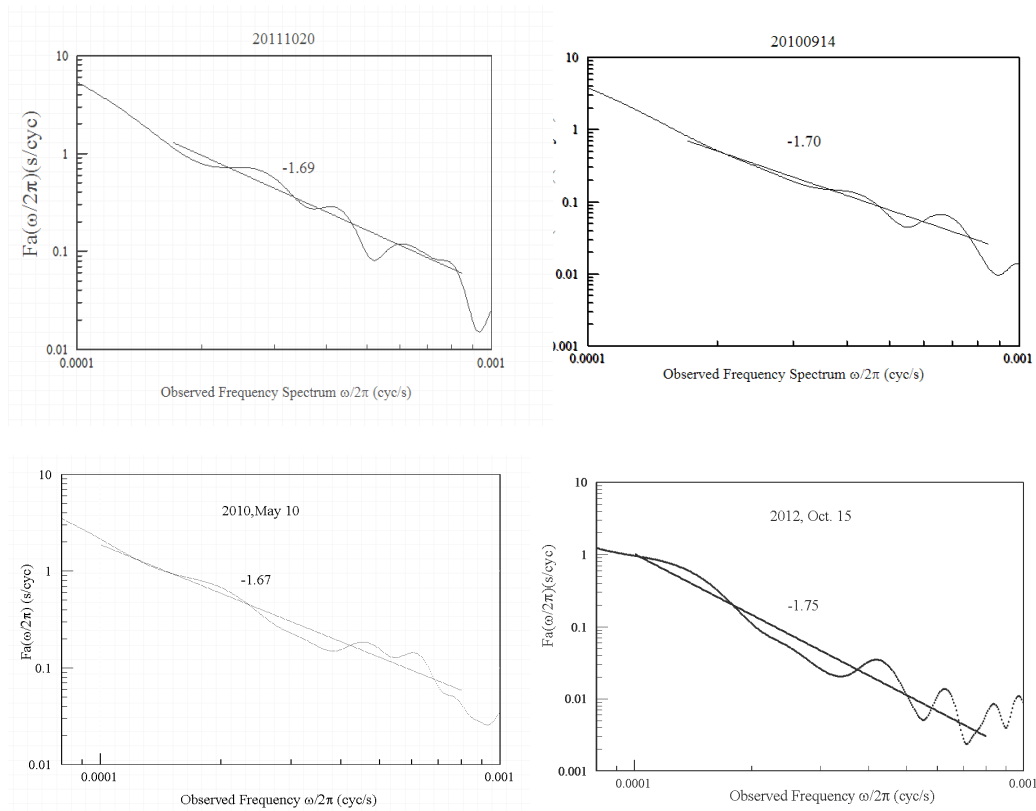


Figure S6. Selected $F_a(\omega)$ and their fitting slope to the spectra of GW atmospheric density perturbations nightly at **Beijing**. The straight dotted lines are the regression fits to the spectra.

Similarly, Figure S6~S8 shows four typical individual examples of the observed frequency spectra at Beijing, Hefei and Hainan.

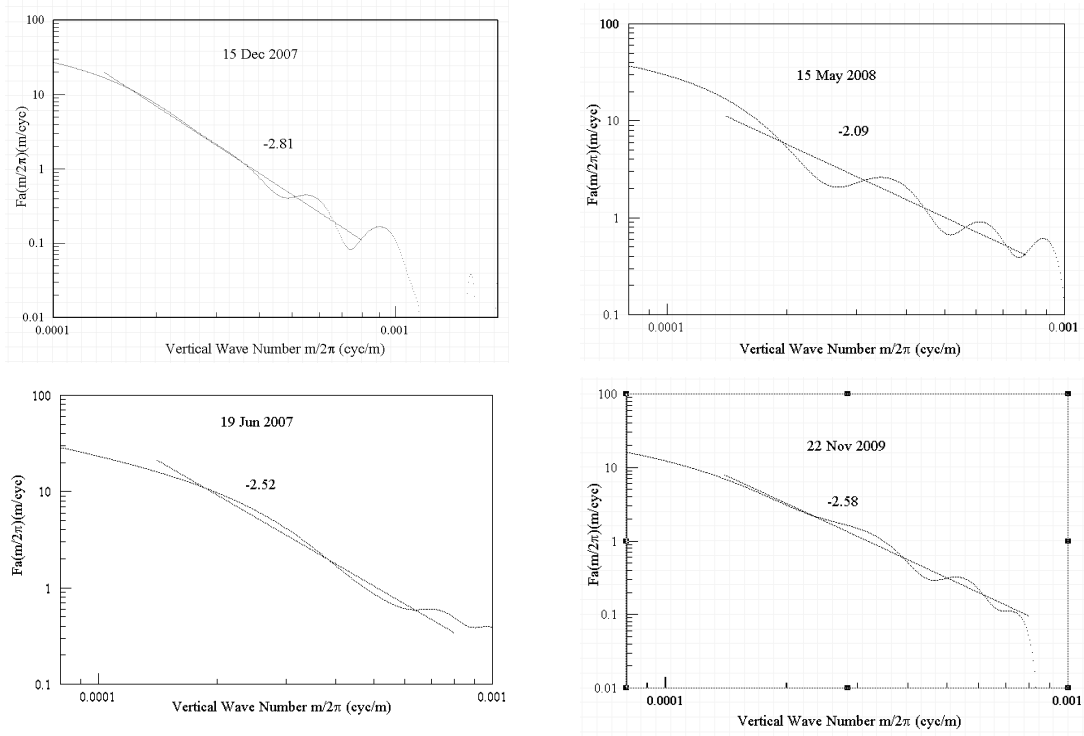


Figure S7. Frequency spectra Vertical wave number power spectra of atmospheric density perturbations associated with gravity waves in the menopause region at **Hefei**.

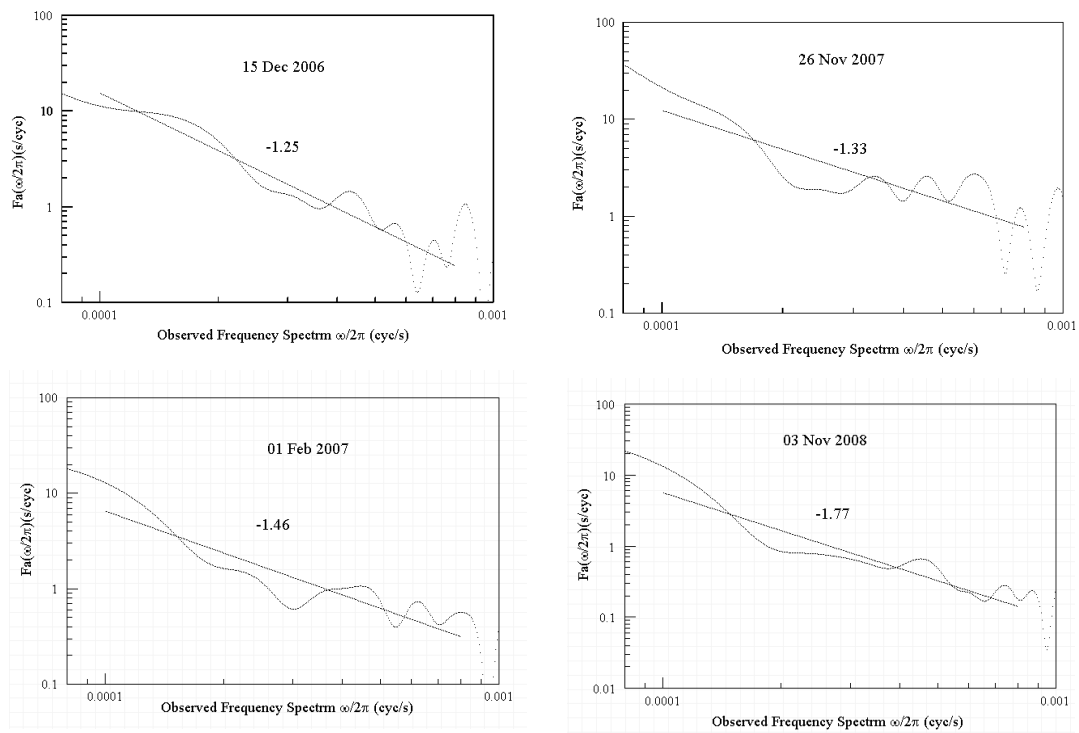


Figure S8. Frequency spectra of atmospheric density perturbations associated with gravity waves in the menopause region at **Hainan**.

Figure **S9** shows the annual mean observed frequency spectra and their linear fitting. The slope of this fitted annual frequency spectra are at Beijing, Hefei and Hainan are -1.92 , -1.90 and -1.80 respectively, which are similar to other authors' report [Senft and Gardner ,1991;Yang et al. 2006].

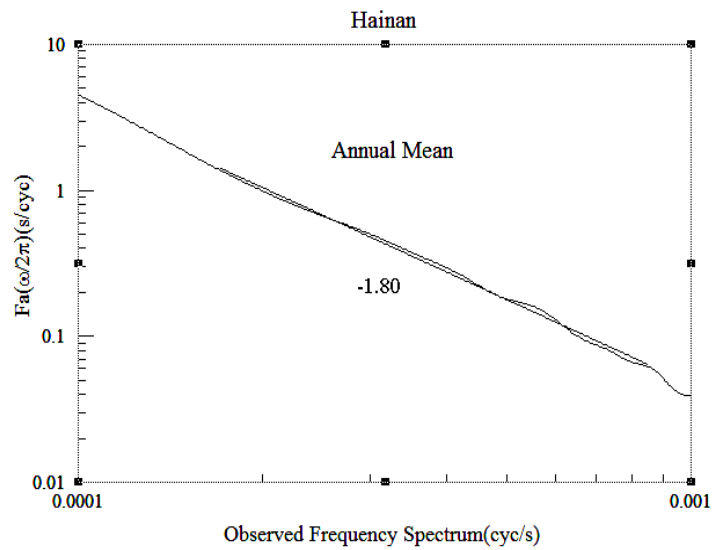
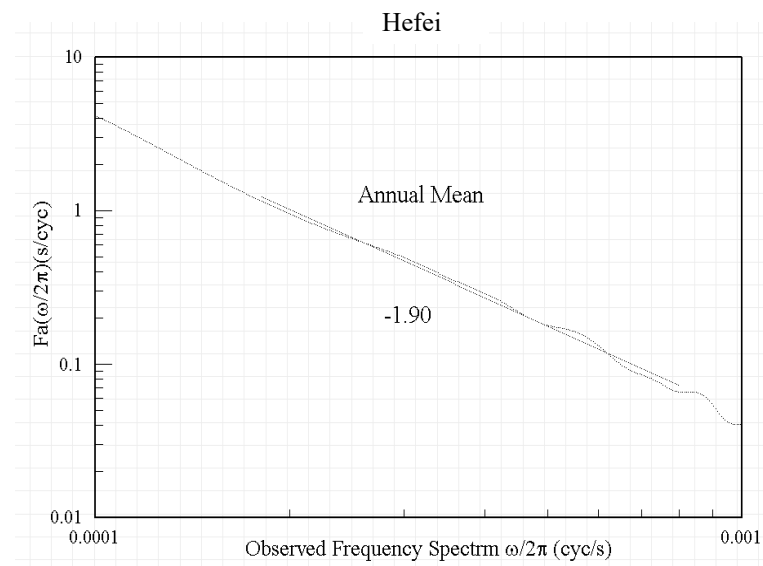
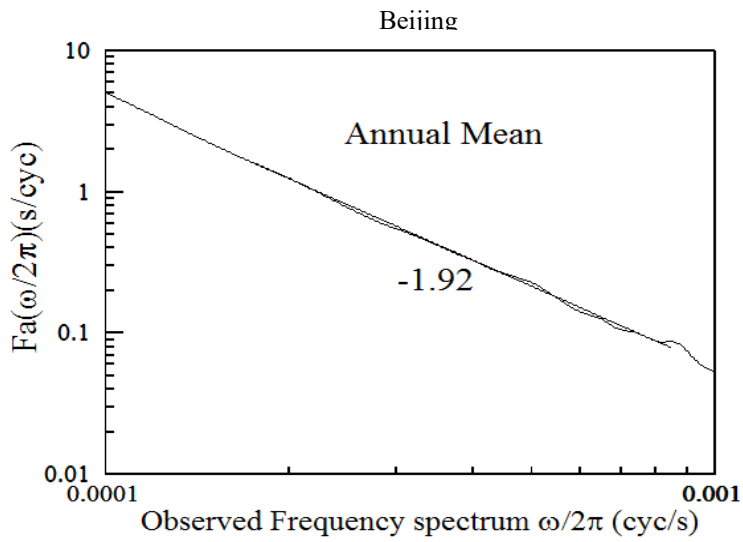


Figure S9. Annual averaged $F_a(\omega)$ and their linear regression fits at Beijing (top), Hefei (middle) and Hainan(bottom).

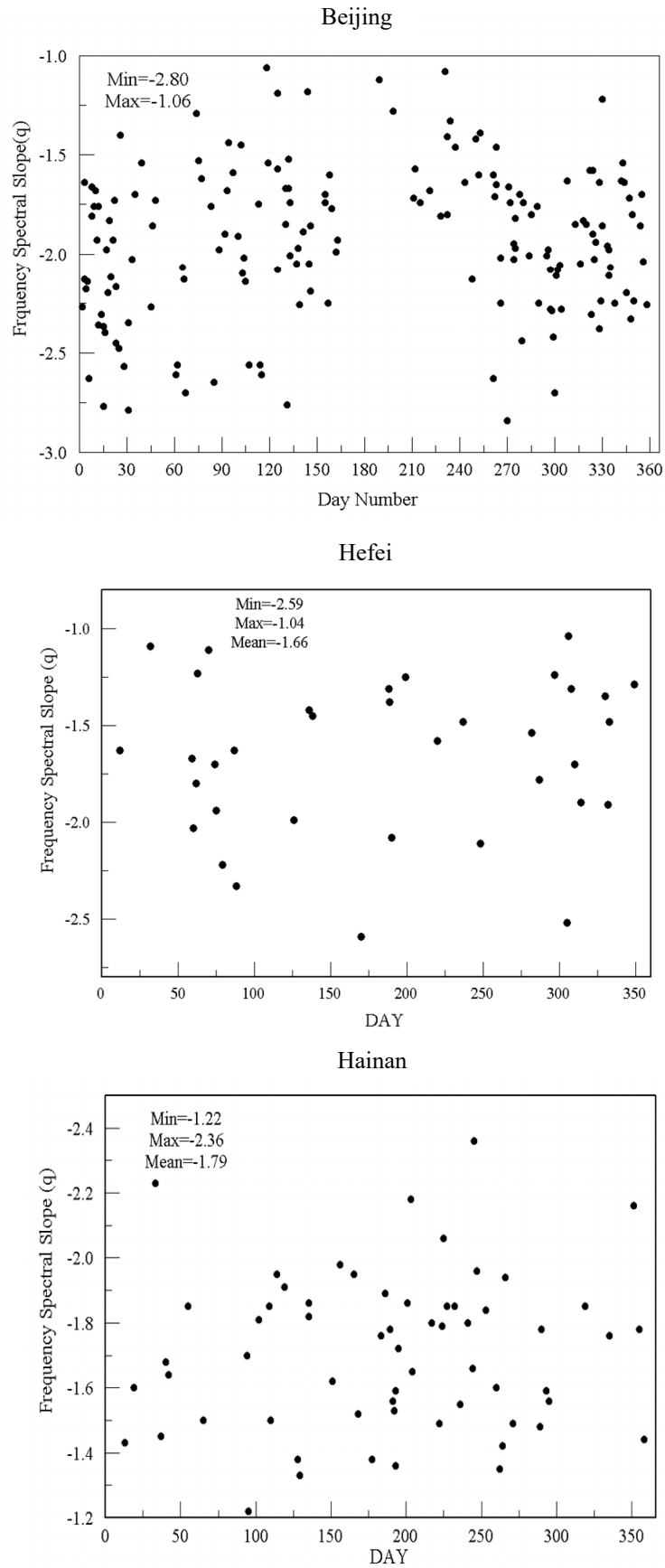


Figure S10. Distribution of fitting slopes of $F_a(\omega)$ at Beijing(top), Hefei(middle) and Hainan (bottom) in statistical seasonally

The annual distribution of the observed frequency spectrum slopes (p) are also shown in Figure S10. At Beijing, the slopes are between -1.06 and -2.80 which cover a range value of 1.74 . Senft and Gardner [1991] have given a relative range value of 1.17 and other authors as Collins et al. [1994], also given the similar result. And our result is larger than those previous reports, which may be caused by Doppler effect due to the existence of background wind. While the data at Hefei and Hainan as indicated in Figure S10 (middle) and (bottom), which are also consistent with the previous reports.

The annual mean slope of $F_a(\omega)$ at the three sites are -1.92 (Beijing), -1.66 (Hefei) and -1.79 (Hainan) respectively, It is worth to mention that because the mean wind have a Doppler effect, the slope of $F_a(\omega)$ cannot be quite appropriate with the theory value $-5/3$, and these results are comparable to the previous observations as, -1.85 as given by [Beatty et al., 1992], -1.7 [Collins et al., 1994] and -1.74 [Senft and Gardner, 1991]), which also seem very reasonable.

Reference:

- Beatty T J, Hostetler C A, Gardner C S. 1992. Lidar observations of gravity wave and their spectra near the mesopause and stratopause at Arecibo. *J. Atmos. Sci.*, 49: 477-496
- Batista, P P., Clemesha, B R, Batista, I S., Simonich D. M. 1989, Characteristics of the sporadic sodium layers observed at 23°S , *J. Geophys. Res.*, 94, 15,349 – 15,358.
- Collins R L, Nomura A, Gardner C S. 1994. Gravity waves in the upper mesosphere over Antarctica: lidar observations at the South Pole and Syowa. *Geophys.*

- Res.Lett., 99:5475-5485
- Dewan, E M, and Good R E 1986, Saturation and the “universal spectrum for vertical profiles of horizontal scalar winds in the atmosphere, *J. Geophys. Res.*, 91, 2742 – 2748.
- Dewan E M. 1994. The saturated-cascade model for atmospheric gravity wave spectra and the wavelength-period (W-P) relations. *Geophys. Res.Lett.*, 21: 817-820
- Hines C O. 1991. The saturation of gravity waves in the middle atmosphere, part 2. Development of Doppler-spread theory, *J. Atmos. Sci.*, 48: 1360-1379
- Senft D C, Gardner C S. 1991. Seasonal variability of gravity wave activity and spectra in the mesopause region at Urbana . *J. Geophys. Res.*, 96, 17229-17264
- Tsuda, T., T. Inoue, D. C. Fritts, T. E. Vanzandt, S. Kato, T. Sato, and S. Fukao 1989, MST radar observations of a saturated gravity wave spectrum, *J. Atmos. Sci.* , 46, 2440 – 2447
- Yang G, Clemesha B, 2006. Batista P, Simonich D. Gravity wave parameters and their seasonal variations derived from Na lidar observations at 23°S, *J. Geophys. Res.*, 111, D21107